A Multimodal Human-Robot Interface to Drive a Neuroprosthesis for Tremor Management

J.A. Gallego, *Student Member, IEEE*, J. Ibáñez, J.L. Dideriksen, *Student Member, IEEE*, J.I. Serrano, M.D. del Castillo, D. Farina, *Senior Member, IEEE*, and E. Rocon *Member, IEEE*

***Abstract*—Tremor is the most prevalent movement disorder, and its incidence is increasing with aging. In spite of the numerous therapeutic solutions available, 65 % of those suffering from upper limb tremor report serious difficulties during their daily living. This gives rise to research on different treatment alternatives, amongst which wearable robots that apply selective mechanical loads constitute an appealing approach. In this context, the current work presents a multimodal Human-Robot Interface to drive a neuroprosthesis for tremor management. Our approach relies on the precise characterization of the tremor to modulate a functional electrical stimulation system that compensates for it. The neuroprosthesis is triggered by the detection of the intention to move derived from the analysis of electroencephalographic activity, which provides a natural interface with the user. When a prediction is delivered, surface electromyography serves to detect the actual onset of the tremor in the presence of volitional activity. This information in turn triggers the stimulation, which relies on tremor parameters amplitude and frequency derived from a pair of inertial sensors that record the kinematics of the affected joint. Surface electromyography also yields a first characterization of the tremor, together with precise information on the preferred stimulation site. Apart from allowing for an optimized performance of the system, our multimodal approach permits implementing redundant methods to both enhance the reliability of the system, and adapt to the specific needs of different users. Results with a representative group of patients illustrate the performance of the interface here presented and demonstrate its feasibility.**

***Index Terms*—Neural engineering, Electroencephalography, Electromyography, Sensor Fusion**

I. Introduction

TREMOR is defined as a rhythmical, involuntary oscillatory movement of a body part [1], and can be broadly classified into physiological and pathological tremor. Pathological tremor is an umbrella term that encompasses those tremors that impair motor performance [2], and, as a whole, constitutes the most extended movement disorder (see, e.g., [3]), and its prevalence is increasing with ageing.

The work presented in this paper has been carried out with the financial support from the Commission of the European Union, within Framework 7, specific IST programme "Accessible and Inclusive ICT", Target outcome 7.2 "Advanced self-adaptive ICT-enabled assistive systems based on non-invasive Brain to Computer Interaction (BCI)", under Grant Agreement number ICT-2007-224051, "TREMOR: An ambulatory BCI-driven tremor suppression system based on functional electrical stimulation."

J.A. Gallego, J. Ibáñez, J.I. Serrano, M.D. del Castillo and E. Rocon are with Bioengineering Group, Consejo Superior de Investigaciones Cientficas, CSIC, Spain. Corresponding author email: ja.gallego@csic.es.

J.L. Dideriksen is with Center for Sensory-Motor Interaction, Department of Health Science and Technology, Aalborg University, Denmark.

D. Farina is with Department of Neurorehabilitation Engineering, Bernstein Focus Neurotechnology Goettingen, Bernstein Center for Computational Neuroscience, Georg-August University, Germany.

In spite of the existence of various therapies to manage pathological tremor, 65 % of those suffering from upper limb tremor report serious difficulties when performing their activities of daily living (ADL) [4]. Moreover, pathological tremors –simply referred to as tremors in the remainder of the paper– arise from a number of disorders such as Parkinson's disease or essential tremor, none of which is fully understood [5], which hampers the refinement of current treatment forms.

Amongst the alternative approaches to tremor management that are referred to in the literature, the application of mechanical loads to the affected limbs has emerged as a potential solution [6] [7] [8]. As a matter of fact, the results shown in [8] demonstrated the feasibility of tremor attenuation with a wearable robot, although the patients were reluctant to utilize such a bulky and anesthetic device as a robotic exoskeleton. In this regard, a neurorobot or neuroprosthesis (NP) that artificially drives the affected muscles through electrical stimulation constitutes a promising solution, since it avoids the needs of external actuators, and hence will better fulfill the user's esthetic expectations. In addition, functional electrical stimulation (FES) for tremor suppression has already been preliminarily validated in [7].

This paper presents the design and proof of concept of a multimodal Human-Robot Interface (mHRI) to drive such a system, i.e. a NP to manage upper limb tremor based on the selective application of mechanical loads through FES. The NP is conceived as an assistive device that compensates for the tremor only when it poses a functional problem, therefore accurate characterization of both the volitional movement and the concomitant tremor are required.

To this aim, the mHRI presented here simultaneously assesses the preparation and execution of the movement based on concurrent recordings from the central nervous system, the peripheral nervous system, and the biomechanics of the affected limb. This is performed by simultaneous electroencephalographic (EEG), electromyographic (EMG), and inertial sensor recordings, and provides the patient with a very natural interface that both requires no learning from his/her part, and reacts with a minimum latency when compared to the realization of volitional movement. This maximizes the ease of use, and makes the interface suitable for a larger population. Therefore, our approach to mHRI guarantees that the system will only "assist when needed" based on the detection of intention to move from EEG, which also has positive implications in terms of energy efficiency, and of discomfort and habituation to stimulation.

The other major benefit derived from this concept is that

TABLE I
INFORMATION THAT CAN BE EXTRACTED FROM EACH SENSOR MODALITY TOGETHER WITH THEIR INHERENT DRAWBACKS

	Positive features	Drawbacks
EEG	- Anticipation to movement onset. - Distinction of voluntary movement and tremor.	- Low reliability (false positive and false negative rates). - Uncertain anticipation time in a single trial analysis ($[\sim 2 - 0]$ s) - Some subjects do not present recognizable patterns to be classified. - Challenging to use concurrently with FES.
sEMG	- Robust detection of voluntary and tremulous activity. - Fast and accurate detection of tremor. - Direct identification of the tremulous muscles (preferred stimulation sites).	- Challenging to use concurrently with FES (physiological artifacts). - Nonlinear and complex relationship between muscle activation and joint kinematics. - Maximum movement anticipation limited by the electromechanical delay.
Inertial sensors	- Usable with FES (no EMI). - Reliable and accurate parameterization of tremor.	- Delay in detection of voluntary movement and tremor onset (algorithms). - Impossibility to identify the source (muscle) that causes the tremor because it is measured as joint movement and not as muscle activity. - Convergence time of tracking algorithms.

multimodality allows for redundant extraction of the same features, which enhances the overall reliability and performance of the system. The idea here is that at the same time that we exploit the sensor modality that provides the best characterization of a given phenomenon, we implement redundant mechanisms that compensate for misdetections or false positives.

Apart from these considerations that could be contemplated as general to most mHRI-driven NPs, we had to incorporate additional features for our specific case of tremor management. The most important among them are fast response, accurate parameterization of the tremulous movement, and capacity to adapt to slow and fast signal non-stationarities. Fast response is important both because most tremors tend to exhibit a transient stage in which their amplitude increases, and thus can be compensated with less actuation effort if its done during this phase, and because some ADLs involve relatively short movements, and therefore delayed actuation would not provide any functional benefit. Accurate estimation of tremor amplitude and frequency is necessary for precise modulation of the different control strategies that can be exploited to suppress the tremor [9]. Finally, examples of non-stationarity are the changes in EMG due to muscle fatigue [10] [11], or the inherent alterations in the basal rhythms of EEG [12].

The practical implementation of our mHRI faced a number of scientific and technological challenges. Amongst the major scientific challenges were the online detection of movement intention in tremor patients and the real-time characterization of tremor from EMG, which had not been investigated before. Notice that most tremors are originated within brain nuclei [5] [13] [14], which may alter the properties of the EEG signals when compared to those recorded in healthy subjects [15] [16] [17]. As for the online parameterization of tremor with inertial sensors, a number of works are available, as reviewed below. The major technological challenges were those intrinsic to the recording of EEG and EMG, being the most important obtaining a good interface that permits acquiring signals with high signal to noise ratio. Since the current work aims at providing a proof of concept of our mHRI, we used non-invasive technologies based on wet electrodes for both, although the mHRI might be implemented in systems that comprise other types of interfaces.

The state of the art techniques to model tremor in real-time normally exploit a single sensor modality, typically inertial sensors, either accelerometers [18] or gyroscopes [19], or electromyographic recordings [20], although research works on fusion of both technologies have just started appearing [21]. On the other hand, to the authors knowledge there is no system in the literature similar to what we propose here, in the sense of employing a mHRI that exploits movement anticipation to drive, based on neural and kinematic information, a NP that compensates for a certain movement disorder or that is aimed at rehabilitating patients after a neurological injury.

This paper is organized as follows. Section II presents the rationale and implementation of the mHRI for parameterization of tremor in the presence of voluntary movement, describing the algorithms employed by the different sensor modalities that constitute the interface. Section III describes the experimental protocol, materials and methods employed for its validation, together with the methodology for data analysis, focusing on the metrics for evaluation of the system as a whole, while Section IV summarizes the results of the evaluation of the system with a representative group of users. Finally, the paper ends with a critical discussion of the performance of the system, with special emphasis on the integration of sensor modalities and the implications our results have when driving the tremor management NP, and with conclusions that summarize the major achievements.

II. MULTIMODAL HUMAN-ROBOT INTERFACE TO CHARACTERIZE TREMOR

A. Overview of the Multimodal Human-Robot Interface

The selection of the specific architecture for the mHRI was based on a detailed analysis of the information that can be extracted from each sensor modality available, paying special attention to the benefits and drawbacks for each choice, especially in the presence of FES (see Table I).

We thus decided to employ EEG to detect the preparation of movement as a transparent way to trigger the NP, surface EMG (sEMG) to monitor the onset of tremor in the presence of voluntary muscle activation, and inertial sensors to drive the NP during stimulation.

In more detail, the implementation of the mHRI was as follows (see Fig. 1). The EEG exploited the direct mea-

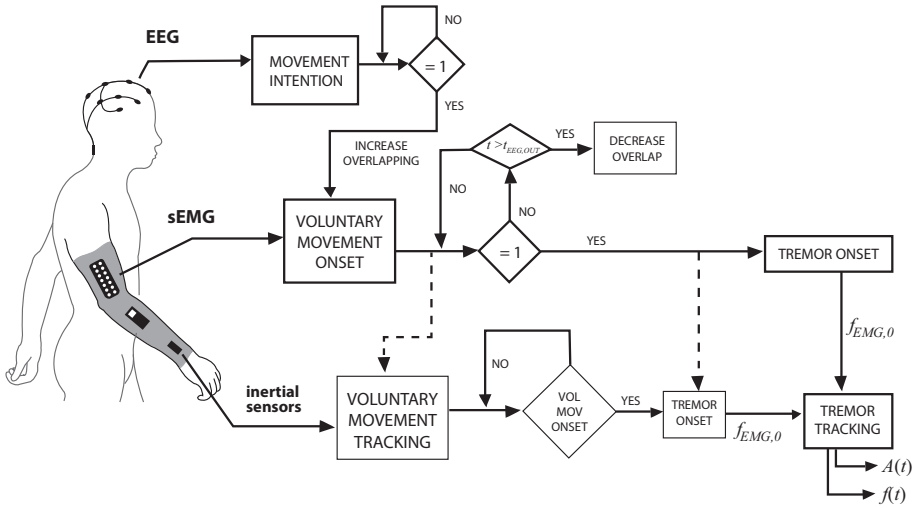

Fig. 1. Diagram that illustrates the mHRI to drive the NP for tremor suppression. The figure shows the normal performance of the system (thick boxes), and the redundant and compensatory mechanisms (thin boxes). Redundant (dashed line) and normal (solid line) flows of information are also differentiated.

surement of the planning of movement in order to naturally trigger the system. However, since the anticipation with which movement can be predicted from ERD analysis varies both between and within subjects [22], a positive detection of movement intention was maintained for a period $t_{\mathrm{EEG,OUT}}$, to guarantee that the sEMG had time to detect the onset of both the voluntary muscle activity and the concomitant tremor. This in turn would trigger the stimulation, which would be modulated based on the instantaneous tremor amplitude and frequency derived from the inertial sensors, because the sEMG is contaminated by the physiological artifacts (the so-called M-wave) that appear due to FES [23]. In addition, sEMG indicated the specific locus of the tremor, a piece of information that would be used by the controller to select the optimal stimulation site, and yielded the tremor frequency of the muscles, which was employed by the inertial sensor algorithm for its initialization.

The EEG algorithm run in overlapping windows (ov_{EEG}) of duration T_{EEG}. At the same time, the sEMG algorithm was executed in windows of duration T_{EMG} and overlapping (ov_{EMG}). The latter was increased to ($ov_{\mathrm{EMG,ho}}$) during the period $t_{\mathrm{EEG,OUT}}$ after a positive detection of the EEG classifier to accelerate the identification of the concomitant voluntary and tremulous muscle activity. Simultaneously, the EEG algorithm went idle, and the voluntary movement filter of the inertial sensors started running, to minimize its settling time. In the presence of tremor, the sEMG algorithm provided the inertial sensors with an estimation of tremor frequency $f_{\mathrm{EMG},0}$ and the stimulation would start.

The integration of different sensor modalities also allowed for the implementation of a set of redundant mechanisms that let the mHRI cope with unexpected conditions, such as misdetections, false positives, et cetera. Three mechanisms, described next, were considered (also see Table I). First, state of the art algorithms for single trial detection of movement intention (from EEG) are not completely accurate, which originates a certain ratio of false negatives that would cause the no actuation of the NP in a situation in which it would be expected to. This was circumvented by using sEMG to detect the onset of both voluntary motion and tremor at the expense, however, of loosing the capability to anticipate with the EEG. Moreover, sEMG compensated for possible false positives of the EEG system, avoiding unnecessary periods of stimulation (see Fig. 1). Second, the appearance of muscle fatigue, a phenomenon that is intrinsic to the execution of relatively long tasks [10], has an important influence on sEMG signals [11], which would alter the thresholds for the detection of tremor and voluntary movement onset. This could be corrected based on the detection of volitional and/or tremulous motion from inertial sensors. Third, the adaptive filters employed to track tremor parameters from inertial sensor information have an inherent settling time (see e.g. [24]) that is almost eliminated by adequate selection of their initial conditions. In this regard, our sEMG algorithm provided the inertial sensors with an accurate estimation of tremor frequency that considerably minimized such convergence time.

Given the intrinsic variability of EEG patterns because of factors such as age [25] or pathology [15], the performance of the classifier here proposed depended on the detection, in each patient, of recognizable patterns associated with the preparation of movement. Patients who did not exhibit these patterns relied entirely on sEMG to detect voluntary movement onset, although the performance of the NP would be degraded. The benefit, on the contrary, is to extend the possible user group to a much larger population.

B. Detection of movement intention from EEG

This algorithm was built to detect movement intention asynchronously, i.e. without any external cue [26], and it thus estimated the probability of identifying a pre-movement condition every period of duration t_{EEG}, at the same time that it avoided the generation of long periods with false activations.

The core of our approach was a single trial identification of the event-related desynchronization (ERD), a neurophysiolog-

ical phenomenon that consists in the decay of the EEG signal power in the mu and lower beta bands over the sensorimotor area, which accompanies the performance of motor tasks [27]. The ERD appears $\sim$ 2 s before the actual onset of the volitional movement, and typically begins over the contralateral hemisphere when movements are performed with the dominant limb [28]. The ERD presents high inter- and intra-subject variability in its spatial and frequency distribution, and therefore we developed an online methodology to choose the best features that describe the pre-movement state in each subject, by training a classifier with the set of most recent movements.

Such features were automatically selected based on the power decrease in the movement state with respect to the basal state, computed in all the channel-frequency pairs available after derivation with a spatial filter. This way the algorithm identified the 3 most significant channel-frequency pairs in terms of movement anticipation, which were used to generate a descriptive model of the pre-movement state by computation of their logarithmic power values.

During execution, a Bayesian classifier was used to decide, based on this model, whether each new data window corresponded to a pre-movement state. The classifier computed independently the probability of the 3 selected features, and combined them to generate the final output. This final output was then compared to a threshold in order to provide the sEMG algorithm with a binary signal that indicated the intention or no intention to move. If the classifier output was positive, it was maintained for the subsequent $T_{\text{EEG,OUT}}$ s, in order to give a stable prediction to the sEMG system, and guarantee the possibility of acknowledging this detection. The threshold was also automatically generated from the training data set, following the optimization criterion of maximization of the movement anticipations while minimizing the number of false positives during intervals of inactivity.

Finally, the EEG classifier used the detection of the voluntary movement to update both its descriptive model and the threshold during execution. This way the classifier always considered the set of most recent movement intervals, reducing the negative influence of the intrinsic non-stationarity of the EEG signal [12] on its performance.

C. Detection of tremor onset from sEMG

We employed a method based on a novel multicomponent AM-FM decomposition technique, the Iterated Hilbert Transform (IHT) [29], to analyze the multichannel sEMG in overlapping windows of duration T_{EMG} (output updated every period t_{EMG}). The IHT consists in the iteration of the Hilbert transformation to a filtered version of the amplitude envelop of the signal. Our approach considered the muscle activity to be a superimposition of the reflections of the voluntary activity (broadband component) and the narrowband oscillations causing the tremor [30]. On the basis of this, the sEMG signal was modeled as the sum of K locally narrowband modulated components according to:

$$Y(n) = \sum_{k=1}^{K} A_k(n) \cos[W_k(n) + P_k(n)] + R_k(n) \quad (1)$$

where n is the sample number, and A, W, P and R the amplitude envelope, the center frequency, the instantaneous phase and the residual respectively.

Applying this method on the tremor sEMG signals, it was shown that the first IHT component consistently reflects the tremor, and that the peak-to-peak amplitude of such component is correlated to the tremor amplitude [30]. Moreover, the level of concomitant voluntary muscle activity can be estimated by subtracting the standard deviation of the tremor component from the offset of this component (low pass filtered, < 2 Hz).

This method was applied to multichannel, high-density, sEMG, which implies that we analyzed information about muscle activity from all parts of the muscle, but with the inherent risk of poor signal-to-noise ratio in a number of the channels. In order to minimize the influence of the latter, the IHT method was applied to each channel individually, and the final estimates of voluntary activation and tremor were obtained as the median value of each parameter from every single channel. These estimates were compared in a final stage to two thresholds defined as follows. The threshold for a significant change in the level of voluntary activity, $th_{\text{EMG,vm}}$, was set to 3 standard deviations above the baseline of the first 5 s of the recording. Tremor amplitude was calculated as the ratio between the RMS of the tremor component and the RMS of the raw, rectified sEMG signal. Significant tremor was defined as being present if this ratio exceeded $th_{\text{EMG,tr}}$.

The final output was thus a pair of binary signals (for each muscle recorded) that indicated the presence or not of voluntary movement and tremor in the analysis window. When tremor onset was detected, the algorithm triggered the actuation of the NP, and provided the inertial sensors with an initial estimation of tremor frequency at the targeted joint, $f_{EMG,0}$. Muscle frequency was translated into joint frequency by simply taking the mean of frequencies of the antagonist muscle pair, in case both exhibited tremor.

D. Parameterization of tremor from inertial sensors

Tremor parameters –instantaneous amplitude and frequency– were continuously estimated with an adaptive algorithm that represented the input signal as a harmonic process based on a truncated Fourier series. The algorithm comprised two filtering stages that were implemented in cascade [31]. First, it removed the no-tremor component of the movement, which is considered to be the voluntary movement given that both are additive [32], and second, it estimated the instantaneous frequency and amplitude of the tremor.

The first stage consisted in a $g - h$ filter that took the raw angular motion $x(n)$ as input, and gave an estimation of the voluntary component of movement, $x_{vm}(n)$, based on the fact that they are separated in frequency [31]. The concomitant tremor, $x_{tr}(n)$, was directly derived from:

$$x(n) = x_{vm}(n) + x_{tr}(n) \quad (2)$$

The second stage of the filter fed the tremor component of movement $x_{tr}(n)$ both into a Weighted Frequency Fourier Linear Combiner (WFLC) [33] that obtained its time-varying frequency, and into a Kalman filter that estimated its instantaneous amplitude, incorporating the tremor frequency obtained by the WFLC in its state model. The Kalman filter implemented a first order truncated Fourier series, where the amplitude terms were updated as random walk models, and the frequency was directly fed from the WFLC. The latter avoided the need of implementing an extended Kalman filter, given that in every sample the state matrix comprised only constant terms. The Kalman filter was formulated as follows:

$$\begin{bmatrix} A_{n,n-1} \\ B_{n,n-1} \\ tr_{n,n-1} \end{bmatrix} = \begin{bmatrix} 1 & 0 & 0 \\ 0 & 1 & 0 \\ \cos(\sum_t \omega_t) & \sin(\sum_t \omega_t) & 0 \end{bmatrix} \begin{bmatrix} A_{n-1,n-1} \\ B_{n-1,n-1} \\ tr_{n-1,n-1} \end{bmatrix} \quad (3)$$

$$y_n = tr_{n,n-1} \quad (4)$$

The process and observation noise were defined as $\mathbf{Q_n} = \text{diag}(\sigma_A^2, \sigma_B^2, 0)$ and $\mathbf{R_n} = \sigma_{tr}^2$ respectively, where the former defined the update of the random walk processes that represented the amplitude terms of the harmonic tremor model, and the latter was related to the noise in the tremor estimated from (3).

The parameterization of tremor derived from this algorithm served to modulate the control strategies that would be implemented in the NP [9].

III. METHODS

A. Experimental protocol

1) Patients: Five essential tremor patients (2 female and 3 male) were included in the study. Age ranged from 47 to 79 years (mean 63.6 $\pm$ 11.9). All patients presented postural and kinetic tremor of mild or moderate severity. Medications were continued at the time of the recordings. All patients signed an informed consent to participate in the study; the Ethical Committee at Universidad Politécnica de Valencia gave approval to the experimental protocol.

2) Protocol: Patients were seated in a comfortable chair during the whole recording session. The experiments consisted in performing a series of exercises that are commonly employed in the clinic to assess tremor. These exercises comprised the so-called finger to finger and finger to nose tests, and elevating both arms and keeping them outstretched against gravity. In total each patient performed 6 repetitions of each exercise. The execution of all the trials followed the same scheme: patients were asked to stay relaxed and keeping the gaze fixed in a wall about 2 m away, and self-initiate the exercise after allowing for a sufficient repose time after the trial started. Total trial duration was 50 s.

3) Recordings: Tremor was recorded from the most affected side both by sEMG and inertial sensors. Surface EMG signals were recorded over the wrist extensors and flexors with a 128-channel amplifier (OT Bioelettronica, Torino, Italy) in differential configuration. The 64-channel array electrode was placed on the muscle belly, and a humidified wrist bracelet served as common reference. The signal was amplified, band-pass filtered (10-500 Hz), and sampled at 2048 Hz by a 12 bit A/D converter. Wrist flexion/extension was measured with two solid-state gyroscopes (Technaid S.L., Madrid, Spain) placed distally and proximally with respect to the anatomical joint, by simply computing their difference [32] [31]. The resultant signal was low pass filtered (< 20 Hz) and sampled by a 12 bit A/D converter at 50 Hz. EEG signals were recorded from 13 positions over the sensorimotor area (FC3, FCz, FC4, C5, C3, C1, Cz, C2, C4, C6, CP3, CPz and CP4 according to the International 10-20 system) with passive Au electrodes. The reference was set to the common potential of the two earlobes and AFz was used as ground. The signal was amplified (g.Tec gmbh, Graz, Austria), band-pass (0.1-60 Hz) and notch filtered (50 Hz), and sampled at 256 Hz by a 16 bit A/D converter. Synchronization of the different systems was controlled by a digital clock signal generated by the computer that recorded inertial sensor data. The data were stored for posterior offline analysis. Only results from those trials with visible tremor are presented here.

B. Data analysis

EEG signals were spatially filtered with a Laplacian filter [34] (5 electrodes: C3, C1, Cz, C2 and C4) or a common average reference (boundary electrodes); no additional preprocessing was done in the sEMG or inertial sensor recordings. Due to the lack of a larger number of trials per patient, we employed a leave-one-out methodology for the training of the EEG classifier.

The parameters of the different algorithms were defined as follows. The output of the EEG algorithm was updated each t_{EEG} = 125 ms based on data from T_{EEG} = 1.5 s windows (ov_{EEG} = 87.5 %), in which the Welch's method with Hanning windows (128 samples, 50 % overlap) was employed to calculate the power spectral density of the signal; positive outputs were maintained for $T_{\text{EEG,OUT}}$ = 2.5 s. The length of the analysis window, T_{EEG}, was selected to be close to the average anticipation of the ERD [27]; the duration of the windows in which it was split (128 samples, 50 % overlap) optimized the trade off between frequency resolution and variance of the estimation. The sEMG algorithm run in T_{EMG} = 1 s windows with overlapping ov_{EMG} = 50 %, and was therefore updated each t_{EMG} = 0.5 s; when the EEG detected the intention to move this value was increased to $ov_{\text{EMG,HO}}$ = 75 %. The threshold for the detection of tremor onset was defined as $th_{\text{EMG,tr}}$= 0.25. The length of the window, T_{EMG}, was selected to ensure that at least two complete oscillations are included within the data to be analyzed with the IHT, and double checked with a previous data set [30]. The overlappings were chosen to keep the computational cost low, allowing for real-time implementation. The inertial sensor algorithm,

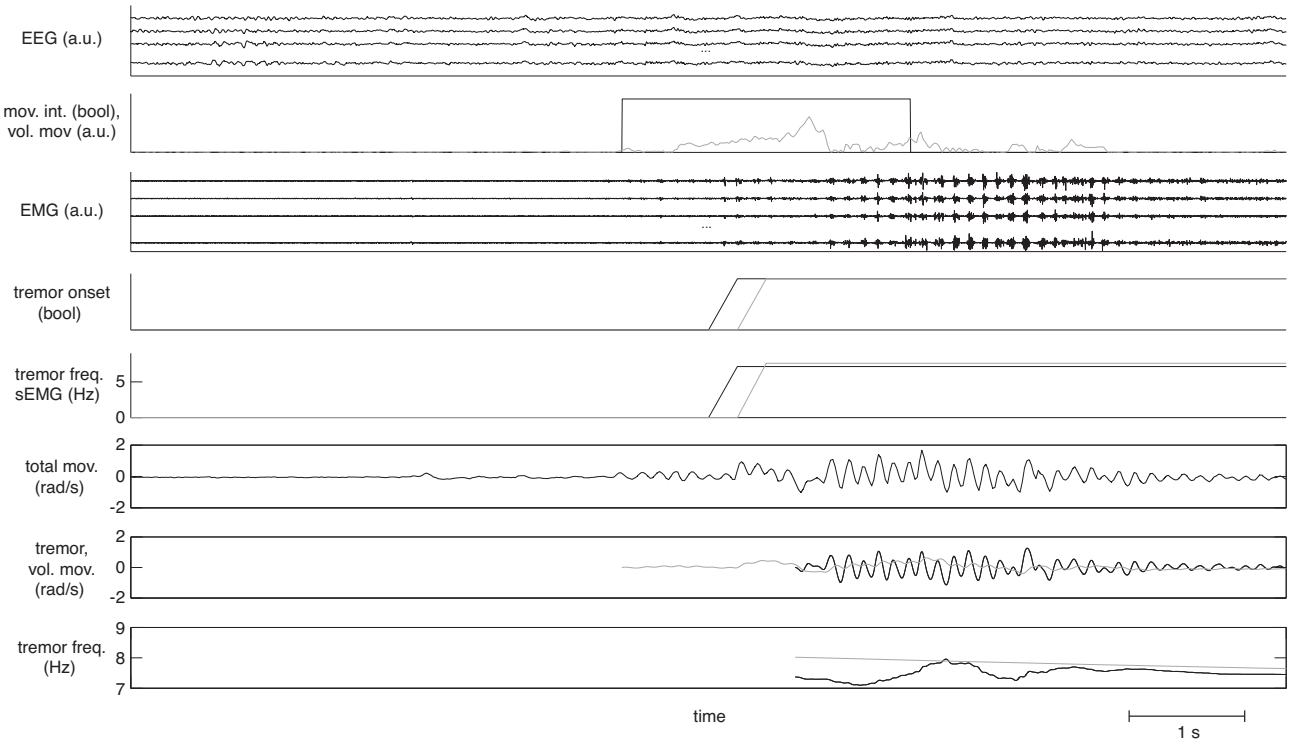

Fig. 2. An example of tremor characterization during a volitional task with the mHRI. The plots show from top to bottom: 1) a few EEG channels, 2) the output of the EEG classifier (black) and the normalized and rectified reference voluntary movement (gray), 3) a few sEMG channels from wrist extensors, 4) tremor onset as detected by sEMG analysis of wrist extensors (black) and flexors (gray), 5) tremor frequency as estimated from sEMG analysis at the time of detection, for wrist extensors (black) and flexors (gray), 6) the raw wrist flexion/extension recorded with inertial sensors, 7) the estimation of tremor (black) and voluntary movement (gray) derived from the inertial sensors, and 8) the tremor frequency estimated from the inertial sensors data (black) and the offline reference (gray).

TABLE II
PERFORMANCE OF THE MHRI

Patient	Movement anticipation (s)	Delay in detection of vol. mov. (s)	Delay in detection of tremor (s)	RMSE tremor amplitude (rad/s)	RMSE tremor frequency (Hz)
01	0.75 ± 0.98	1.40 ± 0.40	0.75 ± 0.43	0.20 ± 0.08	1.20 ± 1.10
02	-	1.83 ± 1.77	1.79 ± 1.91	0.07 ± 0.08	1.36 ± 1.77
03	1.84 ± 1.52	0.78 ± 0.34	0.48 ± 0.61	0.10 ± 0.09	2.92 ± 3.44
04	0.41 ± 0.37	1.17 ± 0.14	1.17 ± 1.14	0.26 ± 0.22	3.22 ± 2.45
05	1.43 ± 1.39	1.03 ± 0.47	1.03 ± 0.98	0.28 ± 0.19	1.41 ± 0.86

updated every sample, used the following parameters, which were conjointly defined for all subjects after examination of a previously recorded data set: i) for the $g - h$ filter, which parameters followed the so-called critically damped relationship [35]: θ = 0.9985, ii) for the WFLC: μ_0 = 2E-5, μ_1 = 1E-3 and M = 1; f_0 was provided by the sEMG algorithm ($f_{\text{EMG},0}$), and iii) for the Kalman filter: σ_A^2 = 1E-7, σ_B^2 = 1E-7 and σ_T^2 = 1E-3.

1) Metrics to assess the performance of the mHRI: The performance of the mHRI as a whole was assessed by computing the anticipation to the movement, the delay in the detection of both voluntary movement and tremor onset, and the error in estimation of tremor amplitude and frequency. These metrics were computed after decomposing the total movement into the reference voluntary and tremor components. The reference voluntary component was obtained by low pass filtering (< 2 Hz, non causal) the input motion, while the remainder gave the reference tremor. Visual inspection in combination with a threshold yielded the onset of both the volitional and tremulous movements, which served to compute the first three metrics. The error in estimation of tremor amplitude was directly computed as the root mean square error (RMSE) between the reference tremor and the output of the inertial sensor algorithm, whereas the error in tremor frequency was calculated as the RMSE between the real frequency (computed in 1 s zero-padded, overlapping windows on the reference tremor) and the output of the inertial sensor algorithm.

In addition, specific metrics were employed to evaluate

TABLE III
PERFORMANCE OF THE EEG CLASSIFIER

Patient	Recall (eTP/NT)	Specifity (%)
01	15/17	96.34
02	-	-
03	11/12	95.35
04	4/6	96.16
05	4/5	85.81

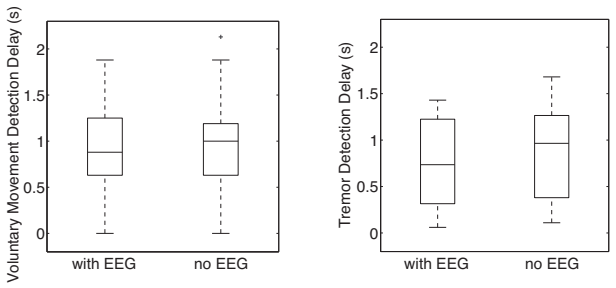

(a) (b)

Fig. 3. Boxplot that summarizes the delay in detection of voluntary movement (a) and tremor (b) from sEMG, with and without the algorithm to detect the intention to move from EEG. The results correspond to all patients and trials, and show the median as the central mark in the box, the 25$^{\text{th}}$ and 75$^{\text{th}}$ percentiles as the edges of the box, the most extreme data points not considered outliers as the length of the whiskers, and the outliers (+).

certain features of the EEG and sEMG algorithms. The performance of the detector of movement intention was evaluated according to the ratio of actual movements anticipated (Recall), and the ratio of false activations during rest periods (Specificity). These metrics used an event-based evaluation due to the fact that our classifier worked asynchronously, and to the slower dynamics of EEG when compared to the classification rate [26] [36] [37]. This way, an event (activation unit, AU) referred to a set of consecutive classifier outputs that are above the decision threshold; an AU was considered an event-based true positive (eTP) when it intersected the interval $[-0.5, 0]$ s (movement onset is at t = 0); otherwise it was treated as an event-based false positive (eFP). The Recall and Specificity were thus defined as:

$$\text{Recall} = \frac{eTP}{NT} \tag{5}$$

$$\text{Specificity} = \frac{\text{length}(\sum eFP)}{\text{length}(\sum \text{rest})} \tag{6}$$

where NT is the number of total movements, and length($\sum eFP$) and length($\sum$ rest) stand for the length of all the eFP and rest periods respectively.

The precision of the initial estimation of tremor frequency derived from sEMG was evaluated by comparing the RMSE between it and that obtained from the amplitude spectrum of the reference tremor (also computed from the reference tremor in a 1 s window with zero-padding). Furthermore, the improvement of initializing the inertial sensor algorithm at tremor frequency derived from sEMG ($f_{\text{EMG},0}$) was assessed by comparing its estimation with that obtained when f_0 = 5 Hz was assumed (as done, e.g. in [33]).

IV. RESULTS

The plots in Fig. 2 show a representative example of the mHRI. The plot depicts both, the raw signals acquired by the different sensor modalities that constitute it (the first, third and sixth plots), and how the different algorithms were triggered and executed. First, the EEG classifier (second plot) predicted the intention to move (anticipation time 0.44 s). This triggered two events: i) the EEG classifier went idle for 2.5 s, and ii) the overlapping of the analysis windows of the sEMG algorithm was increased. During this interval, the sEMG algorithm detected the onset of tremor in the presence of concomitant voluntary activity (fourth plot), and yielded an estimation of tremor frequency (fifth plot). At this moment, the NP would begin to actuate, relying entirely on the tremor parameters derived from the inertial sensors –instantaneous amplitude (the estimated tremor is shown in the seventh plot) and frequency (eight plot)– to modulate its control action. Notice that the inertial sensor algorithm was initialized to the tremor frequency provided by the sEMG.

Table II summarizes the performance of the mHRI in all the patients and trials. No movement anticipation is given for Patient 02, since he did not exhibit visible ERD, and was thus not suited for using the EEG to trigger the system. Therefore, in this case the mHRI entirely relied on sEMG to detect the onset of voluntary movement and tremor, without the prediction derived from the EEG classifier. In summary, the results indicate that the mHRI was capable of consistently anticipating the intention to move (in those patients that exhibited ERD), and that the onset of tremor in the presence of concomitant voluntary movement was rapidly detected (average delay for all patients was 1.11 $\pm$ 1.39 s for voluntary movement detection, and 0.76 $\pm$ 0.45 s for tremor detection), and hence the NP would start assisting with short delay. Moreover, the delay in the detection of both voluntary movement and tremor was considerably increased in the patient without EEG-based movement anticipation (average delay 1.83 $\pm$ 1.77 s and 1.79 $\pm$ 0.91 s for the voluntary activity and the tremor respectively) when compared to the other patients (average delay in all trials 0.88 $\pm$ 0.45 s and 0.77 $\pm$ 0.45 s for the voluntary activity and the tremor respectively). Accurate tracking of tremor amplitude (average RMSE 0.18 $\pm$ 0.17 rad/s) and frequency (average RMSE 2.32 $\pm$ 2.64 Hz) was achieved, and importantly for the controller, with almost zero phase. As a matter of fact, the average delay of the tremor estimation with respect to the offline reference is $3{\cdot}10^{-4} \pm 6{\cdot}10^{-4}$ s, calculated from maximization of the cross-correlation function.

Regarding the movement anticipation, we observed, as expected, notable inter and intra-subject differences (see Table II). However, the EEG classifier provided, for all of them, a good performance in terms of movement anticipated (Recall), and robustness to false activations (Specificity) (see Table III).

We also evaluated what was the outcome of increasing the overlapping of the windows that the sEMG algorithm used (from the 50 % to the 75 %) when intention to move was

TABLE IV
INITIAL ESTIMATION OF TREMOR FREQUENCY FROM SEMG

Patient	RMSE (Hz)
01	1.29 ± 1.26
02	0.54 ± 0.75
03	0.92 ± 1.15
04	2.81 ± 0.72
05	0.86 ± 0.48

TABLE V
ESTIMATION OF TREMOR FREQUENCY WITH AND WITHOUT SEMG

Patient	RMSE tremor freq. (Hz) –no sEMG	RMSE tremor freq. (Hz) –sEMG init.
01	6.50 ± 1.99	1.20 ± 1.10
02	4.36 ± 2.96	1.36 ± 1.77
03	1.85 ± 0.93	2.92 ± 3.44
04	3.79 ± 3.07	3.22 ± 2.45
05	4.20 ± 2.10	1.41 ± 0.86

detected with EEG. Fig. 3 compares the average delay in detection of voluntary movement and tremor onset with and without that feature. In both cases the improvement was statistically significant (Wilcoxon signed rank test, $p < 0.05$), which highlights the benefit extracted from using the prediction of movement derived from EEG to drive the system.

The other major interaction amongst modalities in the mHRI is that between sEMG and inertial sensors. Table IV shows the average RMSE in tremor estimation from sEMG; this is the value the latter used for initialization ($f_{\text{EMG},0}$). The results demonstrate that an accurate estimation of tremor frequency was derived with short delay after its onset (see Table II). Interestingly, the benefit derived from directly initializing the inertial sensor algorithm to the estimation of tremor frequency derived from sEMG was clearly noticeable when comparing the tracking of frequency (see Table V), and also statistically significant (Wilcoxon signed ranked test, $p < 0.05$). Amplitude tracking, on the contrary, was not improved. It must be noticed that the patient that showed the worst performance (Patient 04) had a very mild tremor, and thus it was harder for the system to characterize its features. Also for this patient, the difference between initializing the inertial sensor algorithm at the frequency indicated by the sEMG and not was smaller.

V. DISCUSSION

The results here presented constitute a proof of concept of our approach to a mHRI that predicts the user's intention to move, and detects and parameterizes the concomitant tremor in order to drive a NP for tremor management through FES. This is achieved based on the integration of EEG, sEMG and inertial sensor recordings.

The mHRI constitutes, mainly thanks to the movement anticipation provided by the EEG analysis, a natural interface that requires no learning from the user, because it triggers the NP based on the same mental process that he/she performs to execute a voluntary movement. This has also the additional benefit of encouraging user involvement [38]. Apart from this, the integration of EEG within the mHRI shortens the reaction time of the system (see Fig. 3), which has obvious implications during tremor compensation. There are nevertheless, two scenarios in which the mHRI needs to overcome the absence of this information. The first of them is those patients that present not classifiable ERD, where the sEMG algorithm can assume its role introducing a larger overall delay (as for Patient 02, see Table II). This result implies that those patients that present, for example, a certain neurological condition that impedes the identification of such patterns, can also employ the NP to manage their tremor. The second scenario obviously is a misdetection of the EEG classifier, in which case the same sEMG mechanism is used. As a matter of fact, this idea of enhancing the reliability of the NP constitutes the rationale for always running the sEMG classifier in parallel. It must be noticed, however, that the number of false negatives of the EEG classifier is remarkably low (see Table III). It is also worth mentioning that the overlapping of the sEMG windows could be increased more, which would yield a faster detection of both voluntary muscle activity and tremor. The value selected here was simply chosen to validate the interest of the approach, while ensuring low computational burden.

As for the population who might benefit from the mHRI implementing the EEG, no general inclusion criteria can be defined a priori based on either the literature and/or our experimental results. Although one expects elderly people to exhibit altered spatiotemporal patterns of ERD when compared to their young counterparts [25], the spatial distribution of ERD found in our patients was highly heterogeneous, and did not permit extracting any general conclusion; neither did any particular condition of Patient 02, who showed no classifiable ERD. Nevertheless, abnormalities in synchronization and desynchronization of the motor rhythms have been found both for Parkinson's disease [39] and essential tremor [15], which could hinder the implementation of accurate and reliable EEG classifiers for these patients. As a matter of fact, the performance of our classifier with healthy subjects is in general better than for tremor patients (see [36] for comparison). This may originate from the fact that most tremors originate at deep brain nuclei, which oscillations are projected to a certain extent to the cortices, e.g. through the thalamocortical loop [14], and hence influence the EEG recordings. Notice however, that the false positives of the EEG classifier have no influence on the performance of the NP, given that it is triggered by the detection of volitional movement in the presence of tremor as detected by sEMG. Regarding the differences amongst patients and tasks, it was observed that the anticipation time during bimanual tasks (the finger-to-nose test, and outstretching the arms) was on average larger than in those movements that involve a single limb. Further research on this specific topic needs to be carried out.

Both the sEMG and inertial sensor analysis performed better when the tremor was more severe. This result constitutes a positive finding, since these patients are the first potential user group of our NP. Frequency estimation from inertial sensors degrades the most, given that it is based on a gradient-descend like method [40]. This also occurred when the tremor appeared and reappeared, which happened in some patients during the

finger-to-nose test, probably due to the change of a postural to a kinetic condition.

As mentioned above, our mHRI constitutes an efficient interface to drive a tremor management robot. We think, moreover, that this approach can be beneficial in other types of interventions, e.g. for stroke therapy [38], in order to maximize user involvement and provide the most natural interface to restore the neural pathways. Moreover, other technologies can be used to record the central and peripheral nervous systems and biomechanics in order to construct similar architectures. This will also be required in order to take systems such as the current mHRI to the point of need (e.g. houses, work). Current advances on wearable EEG systems based on dry electrodes [41] and on ambulatory EMG amplifiers, together with the new implantable interfaces for decoding both brain activity at different scales (for a review see [42]) and multichannel EMG [43] constitute a promising advance towards that goal.

VI. Conclusions

This paper presented the design and proof of concept of a mHRI to drive a tremor management NP during voluntary movements. Our mHRI monitors the whole neuromusculoskeletal system through EEG, sEMG and inertial sensor information in order to attain a natural and reliable interface for the NP. This way, the mHRI detects the intention to move in order to provide a fast compensatory action once the user initiates a movement, and when it detects the actual onset of the tremor (in the presence of concomitant voluntary motion), provides the controller with the instantaneous tremor amplitude and frequency, which are employed to drive the stimulation.

Evaluation with a group of 5 patients yielded considerable movement anticipation (while maximizing the number of detections and keeping the false alarms to a low level) and low latency in the effective detection of voluntary and tremulous muscle activity. Moreover, accurate continuous estimation of tremor parameters from inertial sensors is obtained, improved by the information derived from the sEMG. This work therefore demonstrates the interest of evaluating a neuroprosthetic solution to tremor management based on this mHRI.

References

[1] G. Deuschl, P. Bain, and M. Brin, "Consensus statement of the movement disorder society on tremor. ad hoc scientific committee." *Mov Disord*, vol. 13 Suppl 3, pp. 2–23, 1998.

[2] J. H. McAuley and C. D. Marsden, "Physiological and pathological tremors and rhythmic central motor control," *Brain*, vol. 123, pp. 1545–1567, 2000.

[3] G. K. Wenning, S. Kiechl, K. Seppi, J. Müller *et al.*, "Prevalence of movement disorders in men and women aged 50-89 years (bruneck study cohort): A population-based study," *Lancet Neurology*, vol. 4, pp. 815–820, 2005.

[4] E. Rocon, J. M. Belda-Lois, J. M. Sanchez-Lacuesta, and J. L. Pons, "Pathological tremor management: Modelling, compensatory technology and evaluation," *Technology and Disability*, vol. 16, pp. 3–18, 2004.

[5] R. Elble, "Tremor: clinical features, pathophysiology, and treatment," *Neurologic Clinics*, vol. 27, pp. 679–695, 2009.

[6] B. D. Adelstein, "Peripheral mechanical loading and the mechanism of abnormal intention tremor," Master's thesis, Massachusetts Institute of Technology, 1981.

[7] A. Prochazka, J. Elek, and M. Javidan, "Attenuation of pathological tremors by functional electrical stimulation. i: Method." *Ann Biomed Eng*, vol. 20, pp. 205–224, 1992.

[8] E. Rocon, J. M. Belda-Lois, A. F. Ruiz, M. Manto *et al.*, "Design and validation of a rehabilitation robotic exoskeleton for tremor assessment and suppression," *IEEE Tans Neural Syst Rehab Eng*, vol. 15, pp. 367–378, 2007.

[9] J. A. Gallego, E. Rocon, J. Ibáñez, J. L. Dideriksen *et al.*, "A soft wearable robot for tremor assessment and suppression," in *Proc. IEEE Int Robotics and Automation (ICRA) Conf*, 2011, pp. 2249–2254.

[10] S. C. Gandevia, "Spinal and supraspinal factors in human muscle fatigue." *Physiol Rev*, vol. 81, pp. 1725–1789, 2001.

[11] J. L. Dideriksen, D. Farina, and R. M. Enoka, "Influence of fatigue on the simulated relation between the amplitude of the surface electromyogram and muscle force." *Philos Transact A Math Phys Eng Sci*, vol. 368, pp. 2765–2781, 2010.

[12] P. Shenoy, M. Krauledat, B. Blankertz, R. P. N. Rao, and K.-R. Mller, "Towards adaptive classification for bci." *J Neural Eng*, vol. 3, pp. R13–R23, 2006.

[13] F. Steigerwald, M. Ptter, J. Herzog, M. Pinsker *et al.*, "Neuronal activity of the human subthalamic nucleus in the parkinsonian and nonparkinsonian state." *J Neurophysiol*, vol. 100, pp. 2515–2524, 2008.

[14] R. J. Elble, "Origins of tremor," *Lancet*, vol. 355, pp. 1113–1114, 2000.

[15] G. Tamás, L. Plvlgyi, A. Takts, I. Szirmai, and A. Kamondi, "Delayed beta synchronization after movement of the more affected hand in essential tremor." *Neurosci Lett*, vol. 405, pp. 246–251, 2006.

[16] M.-K. Lu, P. Jung, B. Bliem, H.-T. Shih *et al.*, "The bereitschaftspotential in essential tremor." *Clin Neurophysiol*, vol. 121, pp. 622–630, 2010.

[17] M. Kinoshita, T. Hitomi, M. Matsuhashi, T. Nakagawa *et al.*, "How does voluntary movement stop resting tremor?" *Clin Neurophysiol*, vol. 121, pp. 983–985, 2010.

[18] K. C. Veluvolu and W. T. Ang, "Estimation of physiological tremor from accelerometers for real-time applications," *Sensors*, vol. 11, no. 3, pp. 3020–3036, 2011.

[19] A. P. L. Bo, P. Poignet, and C. Geny, "Pathological tremor and voluntary motion modeling and online estimation for active compensation." *IEEE Trans Neural Syst Rehabil Eng*, vol. 19, pp. 177–185, 2011.

[20] H. L. Journée, "Demodulation of amplitude modulated noise: a mathematical evaluation of a demodulator for pathological tremor emg's." *IEEE Trans Biomed Eng*, vol. 30, pp. 304–308, 1983.

[21] F. Widjaja, C. Y. Shee, W. L. Au, P. Poignet, and W. T. Ang, "Using electromechanical delay for real-time anti-phase tremor attenuation system using functional electrical stimulation," in *Proc. IEEE Int Robotics and Automation (ICRA) Conf*, 2011, pp. 3694–3699.

[22] B. Blankertz, G. Dornhege, S. Lemm, M. Krauledat *et al.*, "The berlin brain-computer interface: Machine learning based detection of user specific brain states," *Journal of Universal Computer Science*, vol. 12, p. 2006, 2006.

[23] F. Mandrile, D. Farina, M. Pozzo, and R. Merletti, "Stimulation artifact in surface emg signal: effect of the stimulation waveform, detection system, and current amplitude using hybrid stimulation technique," *IEEE Trans. Neural Syst. Rehabil. Eng.*, vol. 11, pp. 407–415, 2003.

[24] C. Vaz, X. Kong, and N. Thakor, "An adaptive estimation of periodic signals using a fourier linear combiner," *IEEE Trans Signal Proc*, vol. 42, pp. 1–10, 1994.

[25] P. Derambure, L. Defebvre, K. Dujardin, J. L. Bourriez *et al.*, "Effect of aging on the spatio-temporal pattern of event-related desynchronization during a voluntary movement." *Electroencephalogr Clin Neurophysiol*, vol. 89, pp. 197–203, 1993.

[26] S. G. Mason and G. E. Birch, "A brain-controlled switch for asynchronous control applications," *IEEE Trans. Biomed. Eng.*, vol. 47, pp. 1297–1307, 2000.

[27] G. Pfurtscheller and F. H. Lopes da Silva, "Event-related eeg/meg synchronization and desynchronization: basic principles." *Clin Neurophysiol*, vol. 110, pp. 1842–1857, 1999.

[28] O. Bai, V. Rathi, P. Lin, D. Huang *et al.*, "Prediction of human voluntary movement before it occurs." *Clin Neurophysiol*, vol. 122, pp. 364–372, 2011.

[29] F. Gianfelici, G. Biagetti, P. Crippa, and C. Turchetti, "Multicomponent am–fm representations: An asymptotically exact approach," *IEEE Transactions on Audio, Speech, and Language Processing*, vol. 15, pp. 823–837, 2007.

[30] J. L. Dideriksen, F. Gianfelici, L. Z. P. Maneski, and D. Farina, "Emg-based characterization of pathological tremor using the iterated hilbert transform," *IEEE Trans. Biomed. Eng.*, vol. 58, pp. 2911–2921, 2011.

[31] J. A. Gallego, E. Rocon, J. O. Roa, J. C. Moreno, and J. L. Pons, "Real-time estimation of pathological tremor parameters from gyroscope data," *Sensors*, vol. 10, pp. 2129–2149, 2010.

[32] E. Rocon, A. O. Andrade, J. L. Pons, P. Kyberd, and S. J. Nasuto, "Empirical mode decomposition: a novel technique for the study of tremor time series," *Med Biol Eng Comput*, vol. 44, pp. 569–582, 2006.
[33] C. N. Riviere, R. S. Rader, and N. V. Thakor, "Adaptive canceling of physiological tremor for improved precision in microsurgery," *IEEE Transactions on Biomedical Engineering*, vol. 45, pp. 839–846, 1998.
[34] B. Hjorth, "An on-line transformation of eeg scalp potentials into orthogonal source derivations." *Electroencephalogr Clin Neurophysiol*, vol. 39, pp. 526–530, 1975.
[35] E. Brookner, *Tracking and Kalman Filtering made easy*. John Wiley & Sons, Ltd, 1998.
[36] J. Ibáñez, J. I. Serrano, M. del Castillo, and L. Barrios, "An asynchronous bmi system for online single-trial detection of movement intention," in *Proceedings of the 32nd Annual International Conference of the IEEE Engineering in Medicine and Biology Society*, 2010.
[37] G. Townsend, B. Graimann, and G. Pfurtscheller, "Continuous eeg classification during motor imagery-simulation of an asynchronous bci," *IEEE Trans. Neural Syst. Rehabil. Eng.*, vol. 12, pp. 258–265, 2004.
[38] M. Gomez-Rodriguez, M. Grosse-Wentrup, J. Hill, A. Gharabaghi *et al.*, "Towards brain-robot interfaces in stroke rehabilitation," in *Proc. IEEE Int Rehabilitation Robotics (ICORR) Conf*, 2011, pp. 1–6.
[39] L. Defebvre, J. L. Bourriez, P. Derambure, A. Duhamel *et al.*, "Influence of chronic administration of l-dopa on event-related desynchronization of mu rhythm preceding voluntary movement in parkinson's disease." *Electroencephalogr Clin Neurophysiol*, vol. 109, pp. 161–167, 1998.
[40] B. Widrow and S. D. Stearns, *Adaptive signal processing*. Prentice Hall, 1985.
[41] L.-D. Liao, C.-Y. Chen, I.-J. Wang, S.-F. Chen *et al.*, "Gaming control using a wearable and wireless eeg-based brain-computer interface device with novel dry foam-based sensors." *J Neuroeng Rehabil*, vol. 9, p. 5, 2012.
[42] M. A. Lebedev and M. A. L. Nicolelis, "Brain-machine interfaces: past, present and future." *Trends Neurosci*, vol. 29, pp. 536–546, 2006.
[43] D. Farina, K. Yoshida, T. Stieglitz, and K. P. Koch, "Multichannel thin-film electrode for intramuscular electromyographic recordings." *J Appl Physiol*, vol. 104, pp. 821–827, 2008.

Juan Álvaro Gallego (M'11) received the Electrical Engineering degree from University of Vigo, Vigo, Spain in 2007, and the M.Sc. in Robotics and Automation from University Carlos III of Madrid, Madrid, Spain in 2010. He is currently a Ph.D. candidate at the Bioengineering Group, Consejo Superior de Investigaciones Científicas (CSIC), Madrid, Spain. His research focuses on the development of human-robot interfaces and neuroprostheses, and on the neurophysiology of healthy and pathological conditions, specially tremor.

Jaime Ibánez received the diploma in Electrical Engineering from the Universidad de Zaragoza, Zaragoza, Spain and received the M.Sc. degree in Bioengineering and Telemedicine from the Universidad Politécnica de Madrid, Madrid, Spain. He is currently a Ph.D. student with the Bioengineering Group, Consejo Superior de Investigaciones Científicas (CSIC), Madrid, Spain. His research interests include the development of asynchronous Brain-Computer Interfaces aiming at detecting and classifying voluntary movements with the upper-limbs in patients suffering from motor disabilities like stroke and tremor.

Jakob Lund Dideriksen (M'10) obtained the M.Sc. degree in Biomedical Engineering in 2009 from the Center for Sensory Motor Interaction (SMI), Department of Health Science and Technology, Aalborg University, Aalborg, Denmark, where he is currently working on his Ph.D. degree. His research focuses mainly on computational modeling of the behavior of the neuromuscular system in healthy and pathological conditions, including pathological tremor.

José Ignacio Serrano received his Ph.D. from the Complutense University of Madrid in 2007. He is with Consejo Superior de Investigaciones Científicas (CSIC) since 2002 where he has actively participated in National and European projects. His research interests include Cognitive Science, Computational Models of Cognition and Human Behavior, Computational and Cognitive Linguistics, Evolutionary Computation, Knowledge Discovery, Data Analysis and BNMI.

María Dolores del Castillo Tenured Scientist, is with Consejo Superior de Investigaciones Científicas (CSIC) since 1984. She got the PhD in Physics by UCM in 1990, and she has actively participated in National and European since then. She is now a senior researcher of the Bioengineering Group. Her research interests include Cognitive Science, Computational Modeling of human behavior, Knowledge Discovery, Machine Learning, Data Analysis and BNMI.

Dario Farina (M'01-SM'09) received the M.Sc. degree in electronics engineering from Politecnico di Torino, Torino, Italy, in 1998, and the Ph.D. degrees in automatic control and computer science and in electronics and communications engineering from the Ecole Centrale de Nantes, Nantes, France, and Politecnico di Torino, respectively, in 2002.

During 2002-2004, he was Research Assistant Professor at Politecnico di Torino and in 2004-2008 Associate Professor in Biomedical Engineering at Aalborg University, Aalborg, Denmark. From 2008 to 2010 he was Full Professor in Motor Control and Biomedical Signal Processing and Head of the Research Group on Neural Engineering and Neurophysiology of Movement at Aalborg University. In 2010 he was appointed Full Professor and Founding Chair of the Department of Neurorehabilitation Engineering at the University Medical Center Göttingen, Georg-August University, Germany, within the Bernstein Center for Computational Neuroscience. He is also the Chair for NeuroInformatics of the Bernstein Focus Neurotechnology Göttingen. He is an Associate Editor of *Medical & Biological Engineering & Computing* and member of the Editorial Boards of the *Journal of Electromyography and Kinesiology* and of the *Journal of Neuroscience Methods*. His research focuses on biomedical signal processing, modeling, neurorehabilitation technology, and neural control of movement. Within these areas, he has (co)-authored approximately 250 papers in peer-reviewed Journals and over 300 among conference papers/abstracts, book chapters and encyclopedia contributions.

Dr. Farina has been the Vice-President of the International Society of Electrophysiology and Kinesiology (ISEK) since 2010. He is the recipient of the 2010 IEEE Engineering in Medicine and Biology Society Early Career Achievement Award for his contributions to biomedical signal processing and to electrophysiology and in 2012 he has been elected Fellow of the American Institute for Medical & Biological Engineering (AIMBE) for his contributions to neurotechnologies. He is an Associate Editor of IEEE Transactions on Biomedical Engineering.

Eduardo Rocon (M'07) was born in 1979 in Vitória, Brazil. He graduated in Electrical Engineer from Universidade Federal do Esprito Santo (UFES) in 2001. From 1999 through 2000 he was research associate at Laboratorio de Automaão Inteligente (LAI) at UFES. He held a CNPq scholarship at UFES from 1999 through 2000. He received a Ph.D. degree in 2006 from the Universidad Politécnica de Madrid. His research activity was awarded with the Georges Giralt PhD Award as the best Ph.D. robotics thesis in Europe and the EMBEC scientific award. He is current a tenure researcher at the Bioengineering Group, Consejo Superior de Investigaciones Científicas (CSIC), Madrid, Spain. His research interests include rehabilitation, neurophysiology, biomechanics, adaptive signal processing, and human machine interaction.